Imaging of Asteroid 433 Eros During NEAR's Flyby Reconnaissance

J. Veverka,[1] P. C. Thomas,[1] J. F. Bell III,[1] M. Bell,[1] B. Carcich,[1] B. Clark,[1] A. Harch,[1] J. Joseph,[1] P. Martin,[1] M. Robinson,[2] S. Murchie,[3] N. Izenberg,[3] E. Hawkins,[3] J. Warren,[3] R. Farquhar,[3] A. Cheng,[3] D. Dunham,[3] C. Chapman,[4] W. J. Merline,[4] L. McFadden,[5] D. Wellnitz,[5] M. Malin,[6] W. M. Owen Jr.,[7] J. K. Miller,[7] B. G. Williams,[7] D. K. Yeomans[7]

During the 23 December 1998 flyby of asteroid 433 Eros, the Near-Earth Asteroid Rendezvous (NEAR) spacecraft obtained 222 images of Eros, as well as supporting spectral observations. The images cover slightly more than two-thirds of Eros (best resolution is ~400 meters per pixel) and reveal an elongated, cratered body with a linear feature extending for at least 20 kilometers. Our observations show that Eros has dimensions of 33 × 13 × 13 kilometers. The volume, combined with the mass determined by the NEAR radio science experiment, leads to a density of 2.5 ± 0.8 grams per cubic centimeter. This relatively high density, and the presence of an extensive linear feature, suggest that Eros may be a structurally coherent body.

The NEAR spacecraft was launched 17 February 1996 on a 3-year journey to Eros (*1*). As described by Yeomans *et al.* (*2*), when a critical burn scheduled for 20 December 1998 was aborted by the spacecraft, the orbital phase of NEAR's mission had to be postponed until February 2000. However, the trajectory was such that a flyby of the asteroid would occur on 23 December 1998. Here, we summarize the major results obtained by NEAR's camera, the multispectral imager (MSI), and the near-infrared spectrometer (NIS) during the flyby and during the approach to the asteroid. The main objectives for the camera and spectrometer during the flyby were (i) to improve knowledge of the asteroid's size, shape, and rotation phase; (ii) to estimate the volume; (iii) to search for satellites; (iv) to provide a preview of large-scale geology; and (v) to assess the albedo and color heterogeneity of the surface.

Systematic observations of Eros against the star background for navigation began on 5 November 1998, and continued at weekly intervals until 14 December and then at daily intervals until 19 December. Eros was first detected as a +5.5 mag unresolved point of light on 5 November. By 19 November, regular light-curve observations extending over a rotation period of Eros (5.27 hours) were initiated, primarily to refine knowledge of Eros' rotational phase. The rotational period and pole direction had been determined from past Earth-based telescopic and radar observations (*3*) (Table 1).

The geometry of the flyby is summarized in Fig. 1. The flyby sequence consisted of 1026 MSI frames exposed between 15:30 and 22:23 UTC on 23 December 1998 (*4*). Images of Eros were obtained between ranges from 11,662 to 3,827 km and over phase angles from 84° to 113° (Fig. 2). The best resolution (363 m per pixel) was achieved at a range of 3827 km, and the lowest resolution was 1.1 km per pixel. The NIS instrument obtained spectra covering the central part of each MSI frame over a wavelength range of 800 to 2500 nm (*5*). Of the 1026 image frames taken during the Eros flyby, 144 are broadband (clear) filter images (centered at 700 nm with a 140-nm width) taken during the satellite searches or during the closest approach mosaics. The remaining 882 images consist of two six-frame, seven-color mosaics and 24 five-frame, seven-color mosaics covering the uncertainty ellipse of Eros's position; 222 frames include all or part of Eros. In the longer wavelength filter images, the image quality was similar to that of previous MSI images of extended objects. However, an increase in scattered light is evident in the shorter wavelength filters, especially in the 450- and 550-nm images. Comparison of images of asteroid 253 Mathilde (taken 27 June 1997), the moon (taken 23 January 1998), and Eros (taken 23 December 1998) shows a factor of 2 to 3 increase in scattered light up to 15 pixels from a source in the Eros images (*6*). The scattering is progressively worse in the shorter wavelength filters.

Our satellite search, consisting of 4 × 4 image mosaics on both the inbound and outbound legs of the trajectory, was designed to cover the entire sphere of gravitational influence of Eros (*7*), estimated to extend about 100 times the asteroid's mean radius (diameter ~1800 km). Each mosaic was obtained using the MSI broadband filter and took 13 min to complete. The inbound mosaic was taken at ~11,300 km and a phase angle of 84°, and the outbound mosaic at 13,300 km and a phase angle of 113°. Approximate spatial resolution was ~1.1 km per pixel. No candidate satellites have been found down to a magnitude of +8.5, corresponding to objects about 50 m in diameter with an albedo of 0.27.

The rotation pole position [right ascension (RA) = 11.3° ± 4°, declination (Dec) = 20.5° ± 4°], determined from 92 measurements of 19 surface features identified in 21 images, is close to that inferred previously from ground-based studies of the light curve (Table 1). It also agrees with an independent determination made from the MSI images by Yeomans *et al.* (*2*).

As suggested by previous radar observations (*8*), Eros has a long curved shape vague-

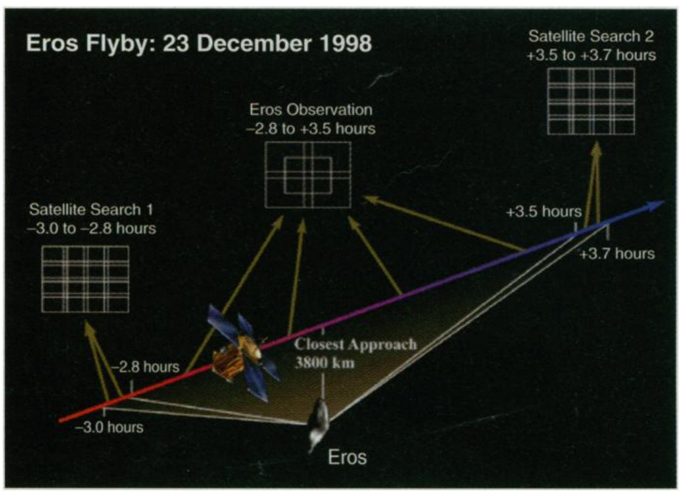

Fig. 1. Schematic timeline of the NEAR flyby on 23 December 1998, summarizing the imaging strategy. The time of closest approach was 18:41:23 UT. The flyby speed was 0.9 km/s. The mosaic modes are indicated.

[1]Space Sciences Building, Cornell University, Ithaca, NY 14853, USA. [2]Department of Geological Sciences, Northwestern University, 309 Locy Hall, Evanston, IL 60208, USA. [3]Applied Physics Laboratory, 11100 Johns Hopkins Road, Laurel, MD 20723, USA. [4]Southwest Research Institute, 1050 Walnut Street, Suite 426, Boulder, CO 80302, USA. [5]Department of Astronomy, University of Maryland, College Park, MD 20742, USA. [6]Malin Space Science Systems Inc., Post Office Box 910148, San Diego, CA 92191, USA. [7]Jet Propulsion Laboratory, 4800 Oak Grove Drive, Pasadena, CA 91109, USA.

ly similar to that of a kidney bean or a banana (Fig. 3). The flyby observations show that the best fit of a triaxial ellipsoid to Eros' nonellipsoidal shape has diameters of 33 × 13 × 13 km, comparable within uncertainties to the estimate of 36 × 15 × 13 km from ground-based data (*9*). Eros is the first asteroid imaged by spacecraft for which a radar shape measurement has also been obtained. The projected dimensions (34.7 × 17.4 km) quoted by Mitchell *et al.* (*8*) agree with those derived from the NEAR images (Table 1). We estimate a volume of 2900 ± 600 km^3 and a mean radius (radius of a sphere of equivalent volume) of 8.8 ± 0.6 km. The greatest uncertainties in the size and shape derive from the fact that high northern latitudes on Eros were not illuminated at the time of the flyby, and that southern latitude limbs were observed at lower spatial resolution than those near and north of the equator.

From the mass reported by Yeomans *et al.* (*2*), our volume yields a mean density for Eros of 2.5 ± 0.8 g/cm^3. This density estimate suggests that Eros may not have the internal porosity of Mathilde, for which Veverka *et al.* (*10*) estimated a porosity of 50 to 80% on the basis of the low mean density of 1.3 ± 0.2 g/cm^3. Although the rock composition of S-type (*11*) asteroid Eros remains uncertain, possible meteoritic analogs range from altered ordinary chondrites (3.3 to 3.9 g/cm^3) to stony irons (4.2 to 5.0 g/cm^3). If chondritic analogs are appropriate for Eros, then the measured

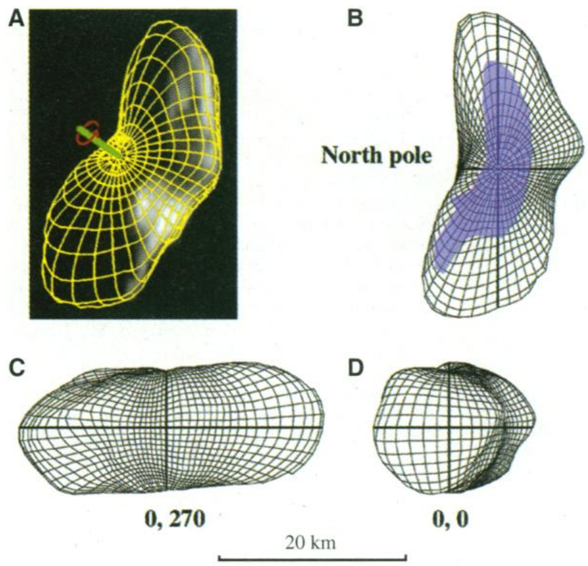

Fig. 3. Pole position and shape model. **(A)** Position of spin pole determined from MSI images. **(B** to **D)** Orthogonal views of the shape model with longitudes measured west from a reference point consistent with the convention used by Murchie and Pieters (*20*). The blue shading in the north polar view (B) delineates the portion of the surface not imaged during the flyby. Longitude 270° (C) shows what is referred to as the "convex" side of Eros in the text. The 0° longitude view (D) corresponds to looking down the long axis of Eros.

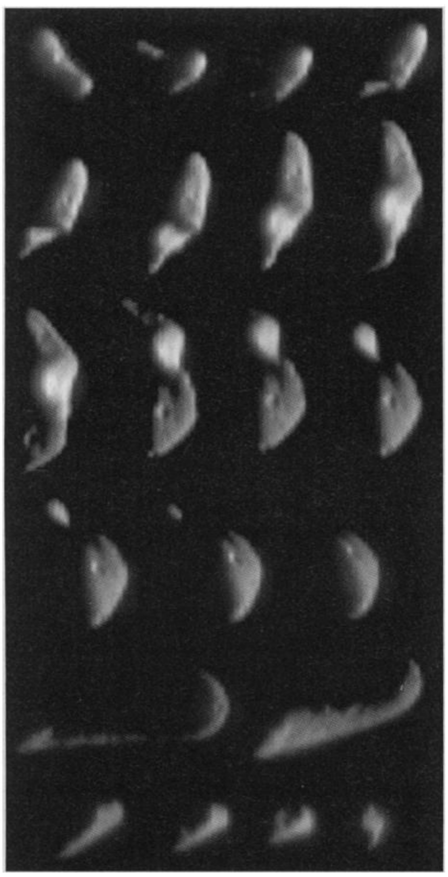

Fig. 2. Representative views of Eros covering 6.6 hours. The phase angle increases from about 84° (top row) to 113° (bottom row). The two elongated images in the fifth row were obtained near closest approach. The resolution varies from ~1 km per pixel (top row) to ~400 m per pixel at closest approach.

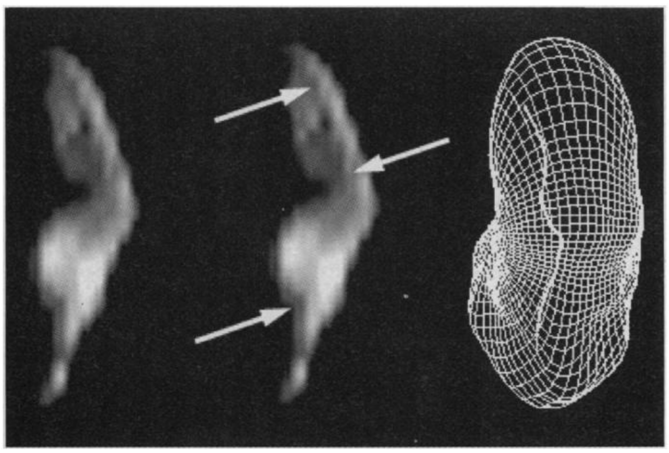

Fig. 4. Linear marking (arrows) identified in image 43732 obtained at a range of 6090 km (resolution ~750 m). The linear marking, possibly a ledge or ridge, can be traced for at least 20 km on Eros (right) and is visible in several other images (see second and third rows of Fig. 2). The presence of this extensive feature suggests that Eros may be a structurally coherent body.

Table 1. Eros parameters.

Ground-based observations	
Orbit	Semimajor axis = 1.45 AU, eccentricity = 0.22, inclination = 10.8°
Spectral type	S-type
Dimensions (*9*)	36 × 15 × 13 (±1) km
Mean radius	9.6 km
Light-curve amplitude	~1 mag
Rotation pole (*9*)	RA = 10.5° ± 2°, Dec = 17.7° ± 2°
Geometric albedo (*21*)	$0.25^{+0.04}_{-0.08}$
Mean density	Unknown
NEAR observations	
Dimensions	33 × 13 × 13 km
Mean radius	8.8 ± 0.6 km
Minimum radius from center of figure	3.9 km
Maximum radius from center of figure	16.4 km
Rotation pole	RA = 11.3° ± 4.0°, Dec = 20.5° ± 4.0°
Volume	2900 ± 600 km^3
Albedo	0.27 ± 0.06
Mean density (*2*)	2.5 ± 0.8 g/cm^3
Surface gravity	0.6 cm/s^2

density allows for porosities ranging from 0 to about 60%. Our current estimate of the density of Eros (2.5 ± 0.8 g/cm^3) is indistinguishable from that of 243 Ida (2.6 ± 0.5 g/cm^3), the only other S-type asteroid for which a mass and density have been determined (*12*).

Small asteroids such as Eros are expected to be either collisional fragments of larger precursor bodies or accumulations of discrete fragments ("rubble piles") (*13*). However, the presence of a linear marking running at least 20 km across the asteroid (Fig. 4) implies that Eros may be structurally continuous. High-resolution views expected during the orbital phase of the mission should reveal whether this apparent linear marking is a ridge, a fault, an exposed layer, or a series of aligned structures.

Five craters can be identified in the images; the two largest, 8.5 and 6.5 km across, have sizes consistent with the maximum crater diameter expected on a body with the dimensions of Eros (*14*). Contrary to the situation observed by NEAR on C-type asteroid Mathilde (*11*), the outlines of Eros are not dominated by a high spatial density of large craters (*10*). The number of craters identified suggests that Eros has a crater density intermediate between the low density of craters observed on asteroid 951 Gaspra and the saturated surface of Ida (*15*). If so, the finding could indicate that Eros is comparatively young, resulting from the disruption of a precursor parent body relatively recently, with insufficient time for its surface to have become saturated with craters once more. Alternatively, the finding could indicate that the cratering record was reset during the formation of one of the large craters. If the detailed measurements expected from the orbital phase of NEAR confirm the suggestion that Eros is a relatively low-porosity body with significant structural continuity, then Eros would be similar to S-type asteroid Gaspra (*16*). NIS spectra show broad similarity to telescopic data (*20*), including evidence for 1- and 2-μm bands. Both features are indicative of pyroxene or olivine, or both.

References and Notes

1. R. W. Farquhar *et al.*, *J. Astronaut. Sci.* **43**, 353 (1995).
2. D. K. Yeomans *et al.*, *Science* **285**, 560 (1999).
3. D. K. Yeomans, *J. Astronaut. Sci.* **43**, 417 (1995); S. J. Ostro *et al.*, *Icarus* **84**, 334 (1990); D. Mitchell *et al.*, *ibid.* **131**, 4 (1998); M. D. Hicks *et al.*, *ibid.*, in press.
4. The sequence began with an inbound satellite search at 15:30 UTC when the spacecraft was 11,672 km from Eros and the solar phase angle was 84°. Near closest approach (3827 km), the goal was to obtain continuous coverage of Eros. Because of uncertainties in the asteroid's position relative to the spacecraft, a large area of the sky had to be imaged to ensure that views of Eros were obtained near closest approach. A sequence was designed that interlaced 2 × 2 mosaics (2 frames across and 2 down) with an additional single frame centered on the most probable position of Eros. Images were taken through seven filters at each position with automatic exposure (*19*). At closest approach, a single 4 × 4 clear-filter mosaic sequence was executed.
5. J. Warren *et al.*, *Space Sci. Rev.* **82**, 101 (1997).
6. During an attitude anomaly that occurred immediately after the aborted burn on 20 December and persisted for 27 hours, more than 28 kg of hydrazine was burned by attitude control jets, creating a diffuse cloud of hydrazine and burn products around the spacecraft. We believe that the enhanced scattering in the Eros flyby images resulted when these materials condensed on the cold outer optics of the imager. Observations of star fields are planned during the remainder of the cruise to Eros to monitor the light-scattering and transmission properties of the camera.
7. Our estimate is based on P. D. Hamilton and J. A. Burns, *Icarus* **92**, 118 (1991).
8. D. Mitchell *et al.*, *ibid.* **131**, 4 (1998).
9. B. Zellner, *ibid.* **28**, 149 (1976).
10. J. Veverka *et al.*, *Science* **278**, 2109 (1997); D. K. Yeomans *et al.*, *ibid.*, p. 2106.
11. S-type asteroids have moderate albedos and spectra, indicating silicates such as olivine or pyroxene. C-type asteroids have low albedos and spectra, indicating carbon or carbonaceous materials on their surfaces [for example, D. J. Tholen and M. A. Barucci, in *Asteroids II*, R. P. Binzel, T. Gehrels, M. S. Matthews, Eds. (Univ. of Arizona Press, Tucson, AZ, 1989), pp. 298–315].
12. M. J. S. Belton *et al.*, *Nature* **374**, 785 (1995).
13. H. Melosh and E. Ryan, *Icarus* **129**, 562 (1997).
14. S. K. Croft, *ibid.* **99**, 402 (1992).
15. For Gaspra, see C. R. Chapman *et al.*, *ibid.* **120**, 231 (1996). For Ida, see C. R. Chapman *et al.*, *ibid.*, p. 77.
16. On the surface of Gaspra, Galileo observed structures of global dimensions (such as planar facets and linear grooves). We note that the specific predictions about the shape of Eros made recently by W. F. Bottke *et al.* (*Astron. J.*, in press) are not supported by the NEAR images. That model considers Eros to be a rubble pile, the shape of which has been influenced by tidal forces during a presumed close passage to Earth.
17. J. Veverka *et al.*, *Icarus* **107**, 72 (1994).
18. For Dactyl, see C. R. Chapman *et al.*, *Nature* **374**, 783 (1995); M. Belton *et al.*, *Icarus* **120**, 1 (1996). For the discovery of Eugenia's moon, see W. J. Merline *et al.*, *Nature*, in press.
19. The MSI camera covers the spectral range from 400 to 1100 nm. For filter specification and nomenclature, see J. Veverka *et al.*, *J. Geophys. Res.* **102**, 23709 (1997). The MSI automatic exposure algorithm is described by S. E. Hawkins *et al.* [*Space Sci. Rev.* **82**, 31 (1997)].
20. S. Murchie and C. Pieters, *J. Geophys. Res.* **101**, 2201 (1996).
21. M. D. Hicks *et al.*, *Icarus*, in press.

22. We thank the Mission Design, Mission Operations, and Spacecraft teams of the NEAR Project at the Applied Physics Laboratory of Johns Hopkins University for their dedicated and vigorous efforts that led to the successful return of key data from the 23 December 1998 flyby. We thank three anonymous reviewers for their comments and suggestions.

16 March 1999; accepted 1 June 1999

Pacemaking the Ice Ages by Frequency Modulation of Earth's Orbital Eccentricity

J. A. Rial

Evidence from power spectra of deep-sea oxygen isotope time series suggests that the climate system of Earth responds nonlinearly to astronomical forcing by frequency modulating eccentricity-related variations in insolation. With the help of a simple model, it is shown that frequency modulation of the approximate 100,000-year eccentricity cycles by the 413,000-year component accounts for the variable duration of the ice ages, the multiple-peak character of the time series spectra, and the notorious absence of significant spectral amplitude at the 413,000-year period. The observed spectra are consistent with the classic Milankovitch theories of insolation, so that climate forcing by 100,000-year variations in orbital inclination that cause periodic dust accretion appear unnecessary.

Understanding the climate of the recent geological past is of importance, because finding out how Earth's environment has transformed the heat input from the sun into climate variations can help predict future global climate change. Most of our knowledge about climatic variations in the Plio-Pleistocene (the last 5.2 million years) is extracted from time series of oxygen isotope ratios, a proxy for global ice volume generally known as the $\delta^{18}O$ records (Fig. 1A). The records show that during the last million years, Earth has experienced at least 10 major glaciations, which according to the astronomical theory of the ice ages (*1*) are the consequence of secular variations in insolation caused by changes in Earth's orbital eccentricity, axial tilt, and longitude of perihelion (Earth's closest approach to the sun). The theory finds support in the fact that the spectra of the $\delta^{18}O$ records contain some of the same frequencies as the astronomical variations (*2–4*), but a satisfactory explanation of how the changes in orbital eccentricity are transformed into the ~100-ky (1 ky = 1000 years) quasi-periodic fluctuations in global ice volume indicated by the data has not yet been found (*5*).

For instance, a fundamental difficulty is to understand the notable absence in the $\delta^{18}O$ data of a significant response to the 413-ky component of the orbital eccentricity, whose signal power is of the same order of magnitude as the 95-ky component. This has been called the "400-ky problem" by Imbrie and Imbrie (*6*).

Department of Geological Sciences, and Wave Propagation Laboratory, University of North Carolina at Chapel Hill, Chapel Hill, NC 27599–3315, USA. E-mail: jar@email.unc.edu